



Effect of calcium addition on microstructure and texture modification of Mg rolled sheets

Han-lin DING¹, Peng ZHANG², Guang-ping CHENG¹, Shigeharu KAMADO³

1. School of Materials Science and Engineering, Anhui University of Technology, Anhui 243002, China;

2. National Engineering Research Center of Light Alloy Net Forming, Shanghai Jiao Tong University, Shanghai 200030, China;

3. Department of Mechanical Engineering, Nagaoka University of Technology, Niigata 940-2188, Japan

Received 23 July 2014; accepted 17 June 2015

Abstract: The mechanical properties and texture of AM60 (Mg–6.0Al–0.3Mn, mass fraction %) and ZXM200 (Mg–1.6Zn–0.5Ca–0.2Mn) Mg alloys subjected to multi-pass hot rolling were investigated. The finer recrystallized grains usually exhibit particular preferred orientations and then alter the total texture feature of rolled sheets. Ca solid solution into Mg matrix serves to the formation of texture component with *c*-axis rotated away from normal direction towards transverse direction and then weakens the overall texture intensity, resulting in a similar anisotropic characteristic to RE-containing Mg alloys.

Key words: Mg sheets; hot rolling; dynamic recrystallization; Ca addition; texture weakening

1 Introduction

Mg rolled sheets, which have the potential for the manufacture of complex parts with thin-walled geometries or large surface areas, can be used in automobile industry and consumer electronics industry due to their excellent mass reduction. However, poor formability at ambient temperature of Mg rolled sheets has limited the development of the secondary forming processes such as sheet stamping and press-forming. The main reason responsible for the formability problem is the formation of typical basal texture (basal planes parallel to the rolled sheet surfaces) during rolling process [1–6]. In this case, the applied stress along with the thickness direction can hardly give rise to the basal and prismatic slips, resulting in the fracture in an initial stage of press-forming at room temperature.

Modifying the texture component or weakening texture intensity should be an effective method to improve the formability of Mg sheets. Consequently, some special processes such as cross-roll rolling [3,4] and differential speed rolling [2,6] have been provided since these methods can impose an intense shear

deformation in the normal direction throughout the sheet thickness. This shear deformation should change the direction of compression stress or induce the occurrence of deformation twinning and then contribute to the modification of texture characteristics.

On the other hand, micro-alloying such as the trace additions of rare earth (RE) into Mg can also promote the texture alteration of Mg sheets. In a previous study, the particle stimulated nucleation (PSN) has also been introduced into Mg alloys as texture randomizing mechanism [7]. However, the observation that PSN is not a necessary precursor to texture randomization has also been demonstrated recently. For instance, the addition of yttrium (Y) [8] and/or RE elements [9,10] also has a significant effect on the texture randomizing, even though there are only very few particles in these alloys. Moreover, recent data from AM60 alloy subjected to large strain rolling show a texture component with basal poles slightly tilted toward transverse direction (TD) [11], a similar texture to that in RE-containing alloys [9], but there are not any RE elements or Y additions into this alloy. Therefore, more work ought to be conducted to clarify the potential influences of PSN and alloying elements on the resulting texture modification.

2 Experimental

In this study, the alloys without RE or Y, AM60 (Mg–6.0Al–0.3Mn, mass fraction %) and ZX200 (Mg–1.6Zn–0.5Ca–0.2Mn) were prepared by an electric furnace under the protection of a mixed-gas atmosphere (CO_2+SF_6). The as-cast billets were homogenized at 424 °C for 24 h to reduce the detrimental effect of eutectic on rollability of these alloys. A multi-pass hot rolling process was carried out under a roll speed of 20 m/min for both alloys. AM60 billet was firstly rolled to a thickness of 2 mm and then further to a final thickness of 0.8 mm at 200 °C. The corresponding rolled sheets were denoted as AM60-2 and AM60-0.8, respectively. ZX200 billet was rolled directly to a final thickness of 0.8 mm at 300 °C. All the rolled sheets were prepared for the examination of the effects of PSN and Ca on texture and deformation behavior of Mg alloys.

The microstructure characteristics were observed on the RD–ND (RD: rolling direction; ND: normal direction) plane of rolled sheets by a field-emission scanning electron microscope (FE-SEM, JEOL JSM–7000F). The micro-texture measurements were conducted by electron back-scatter diffraction (EBSD, EDAX TSL) machine operated at 25 kV. The samples for EBSD were mechanically polished using 100#, 320#, 600#, 1000#, 1500#, 2400# and 4000# grit SiC abrasive papers in conjunction with a water lubricant. The polished samples were then final-polished by 0.04 μm colloidal silica suspension for 40 min following polished by 0.5 μm Al_2O_3 solution for 10 min. A step size of 0.2 μm (approximately 0.3 μm for the minimum grain size measurable) was used for the study of recrystallized grains. The macro-texture evaluations completed with Bruker D8A X-ray diffraction (XRD) were proceeded on a larger region in RD–TD (TD: transverse direction) plane. The element distribution and composition analysis of precipitates in ZX200 alloy were conducted by electron probe micro analyzer (EPMA). The tensile specimens with 4 mm in width and 20 mm in gauge length were machined from each rolled sheet with the angles of 0°, 45° and 90° to rolling direction. The tensile tests were carried out at room temperature with an initial strain rate of 10^{-3} s^{-1} .

3 Results and discussion

Typical stress–strain curves for each rolled sheet examined are shown in Fig. 1. As seen from Fig. 1, AM60-2 sheet exhibits a higher ductility about 25%, but has lower ultimate tensile strength (UTS) and yield strength (YS) as compared with AM60-0.8 sheet, despite the same alloy composition for the two sheets. ZX200

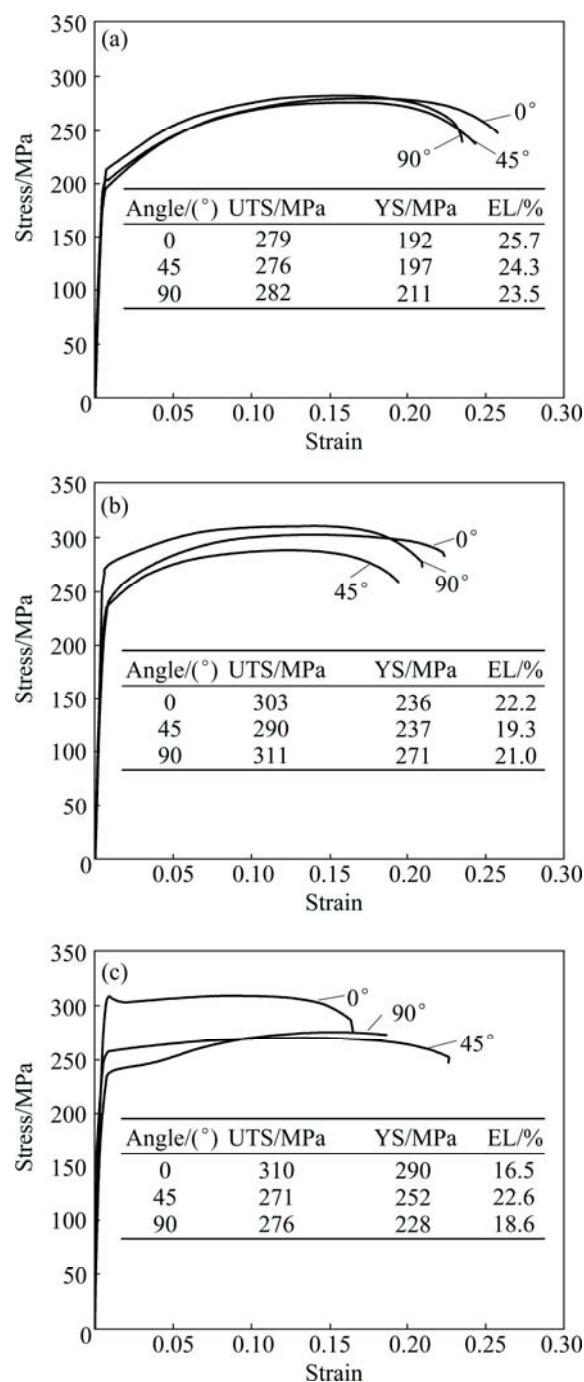


Fig. 1 Stress–strain curves for samples: (a) AM60-2; (b) AM60-0.8; (c) ZX200

alloy has a lower ductility but a higher YS in comparison with AM60 rolled sheets.

Another typical feature from these flow curves is the striking anisotropy in YS and elongation (EL) for the 0°, 45° and 90° oriented samples for all the sheets studied. AM60-2 sheet exhibits a slightly higher EL in 0° direction than in other orientations; however, the YS is the highest for the 90° oriented sample and decreases toward the 0° sample. This result is similar to those observed in alloys AZ31 [12] and ZM21 [9]. Further decrease in sheet thickness has less effect on the

mechanical anisotropy of AM60 rolled sheet, except that the strain-hardening rate along RD appears to be much higher than the other oriented samples in AM60-0.8 sheet. The results obtained from the ZXM200 sheet, however, show an extremely opposite way: the highest YS is measured along 0° and the lowest one is along 90° ; the EL along 45° is significantly higher than other orientations; and more pronounced differences in YS and EL along different directions are apparent. Additionally, ZXM200 sheet shows a rather lower strain-hardening rate than other rolled sheets. It is interesting to note that all these anisotropic characteristics in ZXM200 sheet are very similar to the rolled RE-containing sheets [9].

The macro-texture analyses in RD–TD plane of the present rolled sheets are illustrated in Fig. 2. AM60-2 sheet shows a typical basal texture similar to that observed in the rolled AZ31 alloy [12], in which the (0002) basal plane of the majority of grains is inclined to be parallel to the sheet plane. For AM60-0.8 sheet, the basal poles of some grains have a slight tendency to rotation to RD and TD. It is noted that the tilted rotation of basal pole to RD and TD and then the weakened texture intensity became more pronounced in rolled ZXM200 sheet. This texture characteristics exhibited in rolled ZXM200 sheet also show a similar result to the rolled RE-containing sheets [9]. Furthermore, more obvious tilted rotation toward TD than RD can also be found in Fig. 2(c), which perhaps is a result of more grains having a *c*-axis tilted toward TD or a larger angle of *c*-axis tilted toward TD in rolled ZXM200 sheet. These grains whose *c*-axis is tilted toward TD, when the uniaxial loading is applied along with TD, usually exhibit a larger Schmid factor [13] and then a lower YS due to the easier activation of basal slip. Therefore, this texture characteristic is the primary reason for the rolled ZXM200 sheet showing a different anisotropy of mechanical properties from AM60 sheet.

The present results in our work show that the texture characteristics as well as its mechanical properties exhibited in rolled ZXM200 sheet also show a similar result to the rolled RE-containing sheets [9], although there is no any RE element or Y added into ZXM200 alloy. This raises the question that what has resulted in the formation of this kind of texture in ZXM200 alloy.

The orientation imaging microscopy (OIM) and inverse pole figures (IPF) from EBSD presented in Fig. 3 show the recrystallized grains and their distribution in the rolled sheets. The strong distinctions in these OIM figures are the different amounts of finer grains. Then, the different recrystallized grain sizes related to the amount of finer grains can also be found from the microstructures.

AM60-2 sheet shows an equiaxed fine grain

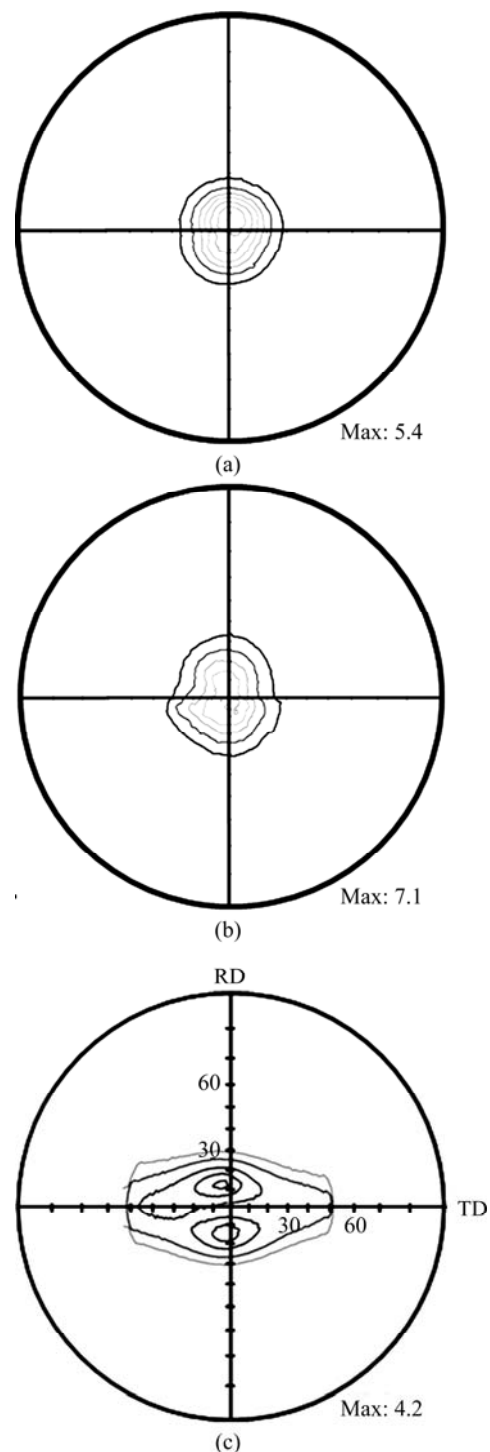


Fig. 2 Macro-texture analyses exhibited by (0002) pole figures for rolled sheets: (a) AM60-2; (b) AM60-0.8; (c) ZXM200

structure with an average size of $3.9\ \mu\text{m}$. For AM60-0.8 sheet, a larger number of finer grains formed during the further hot rolling. As a result, the average grain size is reduced to $3.0\ \mu\text{m}$. The majority of these finer grains have a size less than $1\ \mu\text{m}$, which gives a significant contribution to the decrease in average grain size. If the influence of these finer grains is excluded, a similar grain size ($4.1\ \mu\text{m}$ versus $3.9\ \mu\text{m}$) can be achieved for these

two AM60 sheets. In the case of ZXM200 sheet, the tendency of more pronounced grain refinement gives rise to a smaller average grain size of approximately $1.9\ \mu\text{m}$.

To determine these finer recrystallized grains in rolled sheets, an OIM image with a smaller EBSD step size of $0.1\ \mu\text{m}$ from ZXM200 sheet is illustrated in Fig. 4, and only those finer grains are presented in Fig. 4(b). Additionally, Ca-rich precipitates identified by EBSD software and a few non-indexed pixels could also be found and then illustrated as black regions in Fig. 4(b). This clarifies the fact that almost all the finer grains appear to have nucleated in the vicinity of precipitates.

A comparative analysis from the above EBSD maps illustrates that it is the addition of Ca that results in the formation of finer grains in the rolled sheet and these finer grains have a close relationship with those small particles precipitated during hot rolling. The systematic studies on the second phase particles, Mg_2Ca or $\text{Mg}_6\text{Zn}_3\text{Ca}_2$, and their effect on the mechanical properties of the Ca-addition Mg alloys have been reported [14–16]. In the present ZXM200 alloy, the formation of the second phase particles due to the addition of Ca to Mg–Zn-based alloy can be found in Fig. 5.

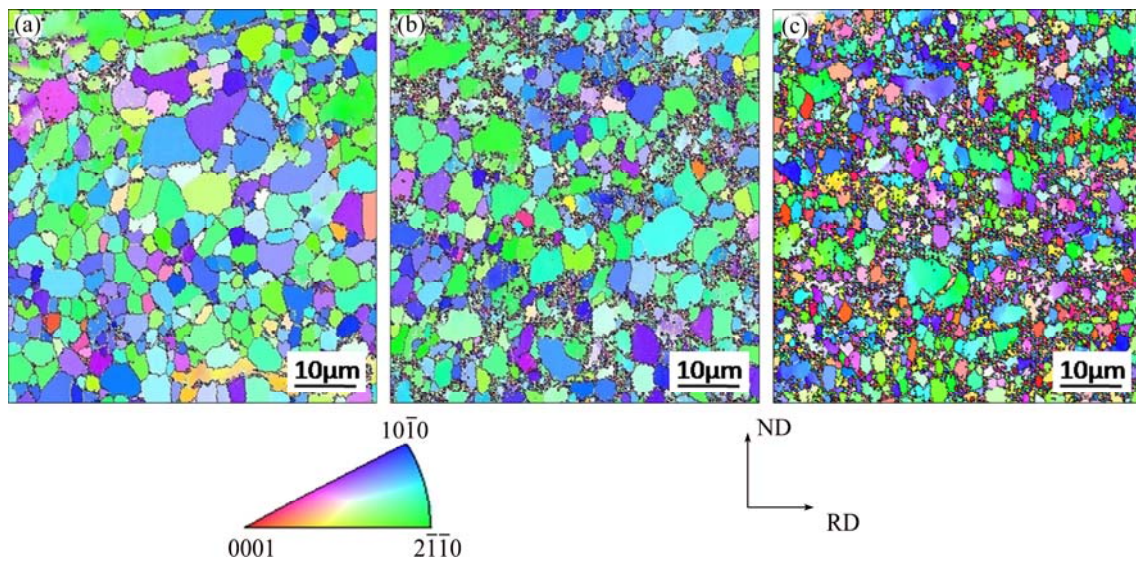


Fig. 3 OIM and IPF maps obtained from EBSD on three sheets: (a) AM60-2; (b) AM60-0.8; (c) ZXM200 (The recrystallized grains are indicated in different colors corresponding to crystallographic orientations indicated in inverse pole figure)

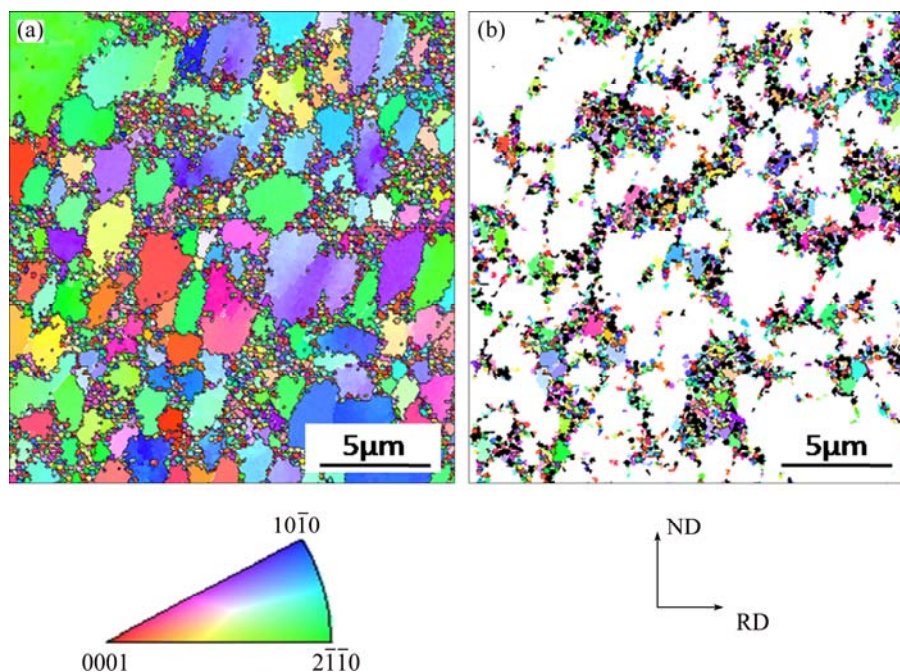


Fig. 4 OIM and IPF maps showing relationship between precipitates and very small grains in ZXM200 rolled sheet: (a) IPF map obtained from EBSD; (b) Precipitates indicated as black regions, large-size grains excluded from IPF map in (a)

EPMA analysis (Fig. 5(a)) shows that Ca element is inclined to be formed Mg–Ca binary phase or Mg–Zn–Ca ternary phase along with the grain boundaries or in global particles inside grains in as-cast alloy. During the hot rolling, some large particles such as those located along with grain boundaries might be broken, and some finer particles would be also precipitated during and/or after hot rolling, as shown in Fig. 5(b). Some DRX grains form in the vicinity of some large particles (shown in the dotted circle region), and many fine precipitates along with the DRX grain boundaries or within the recrystallized grains can also be found, while not all of them are related to classical PSN. This suggests that the formation of these DRX grains might also be achieved by other DRX modes (e.g., by the continuous DRX mechanism or twin-induced DRX) as well as PSN. Whether the recrystallized grains form by PSN or other DRX modes, most of these DRX grains have a grain size of 1 μm .

It is well recognized that only the coarse particles with size greater than 1 μm should contribute to the nucleation of recrystallized grains. Recent results show that the clusters of fine particles can also stimulate the nucleation of new recrystallized grains and would be more effective than single particles, especially under a high strain imposed on the deformed matrix [17,18]. However, most of these fine particles usually exist separately and have a size below 1 μm (Fig. 5(b)). Obviously, the present feature should be not benefit for the occurrence of PSN. On the other hand, those precipitates smaller than 1 μm will restrain the growth of the recrystallized grains by boundary pinning, which is perhaps another reason for the existence of large amount of fine grains.

In order to investigate the effects of the fine recrystallized grains and Ca addition on the texture, the micro-texture analyses based on the EBSD results are

shown in Fig. 6. Similar texture characteristics to XRD measurement can be obtained. For AM60-2 sheet, the peak intensity (I) tilted slightly away from the ND towards RD can also be found in Fig. 6(a). For AM60-0.8 sheet, two marked differences in texture are presented compared with AM60-2 sheet: higher texture strength and formation of the texture component with the basal poles tilted $\sim 15^\circ$ toward TD (indicated as white arrow). The former is ascribed to the fact that more and more grains rotate their basal poles parallel to the ND during the further rolling, while the latter is possibly caused by the lower Al solute content in AM60-0.8 sheet due to the extensive $\text{Mg}_{17}\text{Al}_{12}$ precipitated. However, the as-rolled sheets with lower Al content (e.g., AZ31 [12]) or without Al (e.g., ZM21 [9]) do not have the texture component with $\langle 0001 \rangle // \text{TD}$ at all. Thus, Al content is not the essential reason for this distinct texture. Alternatively, the observed texture alteration may be more closely related to the increase of the amount of finer grains in AM60-0.8 sheet. Although there are also a few finer recrystallized grains in AM60-2 sheet, perhaps the slight number of the finer recrystallized grains is not enough to lead to the texture alteration.

ZXM200 sheet, having much more finer recrystallized grains compared with AM60-0.8 sheet (Fig. 3), exhibits a more significantly different texture from the conventionally typical Mg sheet texture, but an analogous one to that in RE-containing alloys: the texture components with basal poles tilted from ND toward RD or TD are both observed and the spread is significantly broader toward TD than RD; the $(10\bar{1}0)$ planes tend to be perpendicular to the RD; the overall texture strength is lower (Fig. 6(c)). Perhaps the trace additions of Zn and/or Ca elements should contribute to the formation of this kind of texture. Firstly, there is an evidence that a higher Zn solute content has a positive impact on the modification of rolling texture of Mg

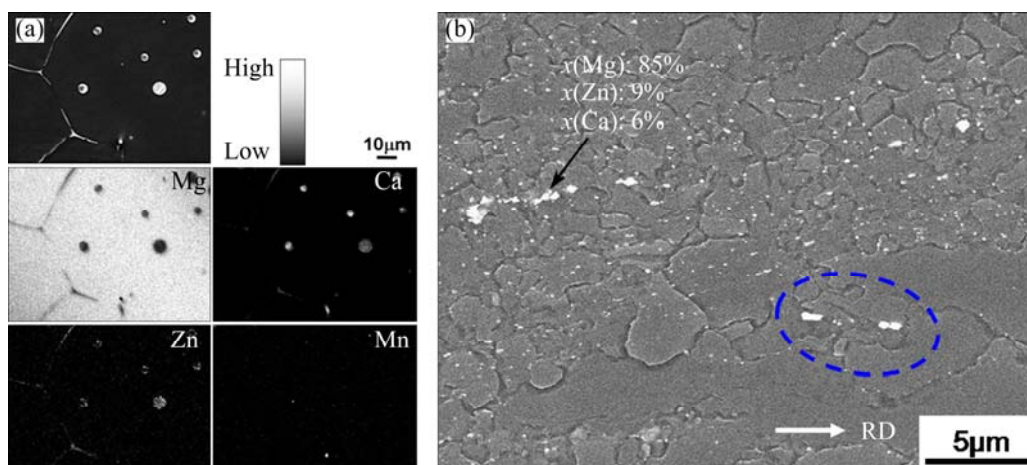


Fig. 5 Particles and Ca distribution in ZXM200 alloy: (a) EPMA analysis for as-cast alloy, indicating local chemical composition of Ca-rich particles; (b) Distribution of particles and their composition analysis in rolled sheet

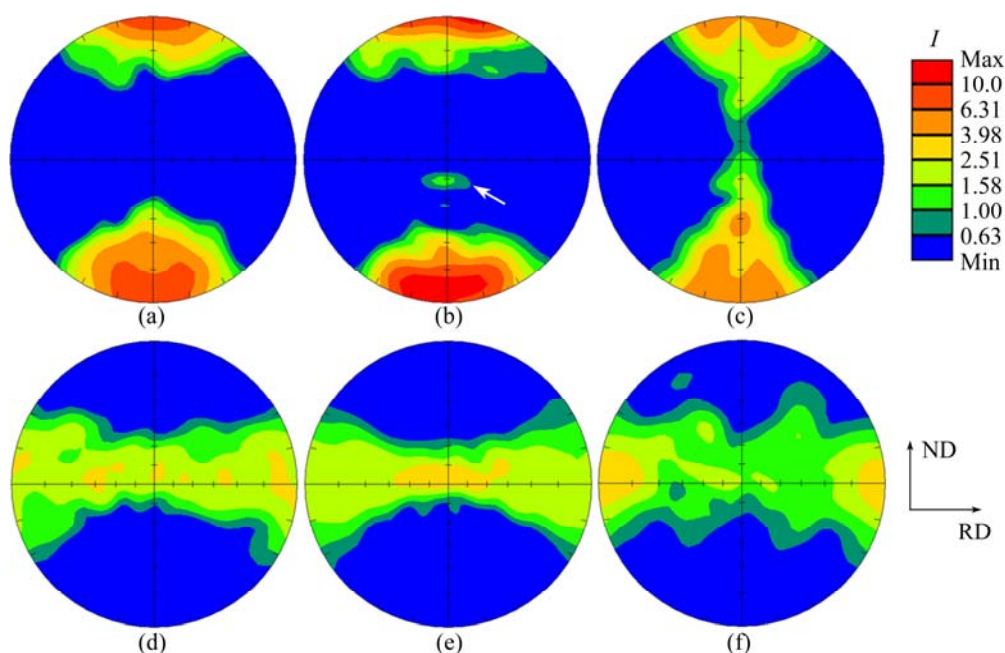


Fig. 6 (0002) (a, b, c) and $(10\bar{1}0)$ (d, e, f) pole figures of rolled sheets: (a, d) AM60-2, $I_{\max}=9.4$; (b, e) AM60-0.8, $I_{\max}=14.2$; (c, f) ZXM200, $I_{\max}=6.2$ (The measurements were proceeded in RD–ND plane and corresponding OIM images can be found in Fig. 3)

alloys [9]. However, due to the formation of second phase [14], the Zn solute content appears to be lower in ZXM200. Secondly, further comparison with ZM21 [9] shows that, in addition to the slight compositional difference of Zn and Mn, the trace addition of Ca into ZXM200 alloy is likely to be the unique distinction, which suggests that Ca addition might have a strong implication for modifying and weakening the texture in this rolled sheet. Of course, the formation of some fine DRX grains might be another possible reason, as observed in AM60-0.8 sheet.

Figures 7(a) and (b) illustrate the grain size distribution in AM60-0.8 and ZXM200 sheets. The grains with the size less than $1\ \mu\text{m}$ have a higher fraction than other grains for both rolled sheets, just similar to the microstructure observations in Figs. 3–5. In order to investigate the influence of these fine grains on texture alteration, the (0002) pole figures were reanalyzed according to the grain size less or greater than $1\ \mu\text{m}$, just as shown in Figs. 7(c)–(f).

It can be seen that the (0002) pole figure of the grains less than $1\ \mu\text{m}$ in AM60-0.8 (Fig. 7(c)) is composed of three main components, i.e., the basal poles are preferentially oriented parallel to TD, ND and RD, as indicated by the different peak intensities; a higher intensity can be observed for the texture component with $\langle 0001 \rangle // \text{TD}$. The phenomenon that the orientations of these peak intensities are all tilted slightly away from the exact direction can also be found. For the large grains in AM60-0.8 sheet, it exhibits a similar basal texture to AM60-2 sheet (Fig. 7(e) vs Fig. 6(a)), indicating that the

texture component with basal poles parallel to TD in AM60-0.8 sheet is primarily a result of these fine recrystallized grains.

Likewise, perhaps we can obtain a similar conclusion from Fig. 7(d) that the texture alteration observed in Mg alloy with Ca addition (ZXM200) is also ascribed to those fine recrystallized grains. However, the (0002) pole figure of the grains greater than $1\ \mu\text{m}$ in ZXM200 (Fig. 7(f)) also shows a distinctive feature from that in conventional Mg rolled sheets even though the influence that those fine recrystallized grains have on the texture alteration has been removed. It is further noted that, in comparison with those finer grains, the large grains exhibit a more similar texture feature to that in RE-containing alloys reported previously. Therefore, it is concluded that Ca solid solution into Mg matrix may also play a dominant role in the weakening of basal texture. This verifies the hypothesis that the Ca addition could modify the basal texture efficiently in Mg alloys and consists with the reported results in Ref. [19]. However, the primary reason why Ca has a similar effect on the texture alteration to RE is not clearly clarified yet. One possible reason may be due to the fact that both Ca and RE elements have a larger atomic size with respect to Mg, while the traditional strengthening additions, Al and Zn, are both smaller than Mg atom. Then the solid solution of Ca atoms results in the occurrence of lattice distortion and the consequent decrease of c/a , which will contribute to the activation of non-basal slip and then weaken the texture characteristics [20].

Generally, PSN is expected to give rise to randomly

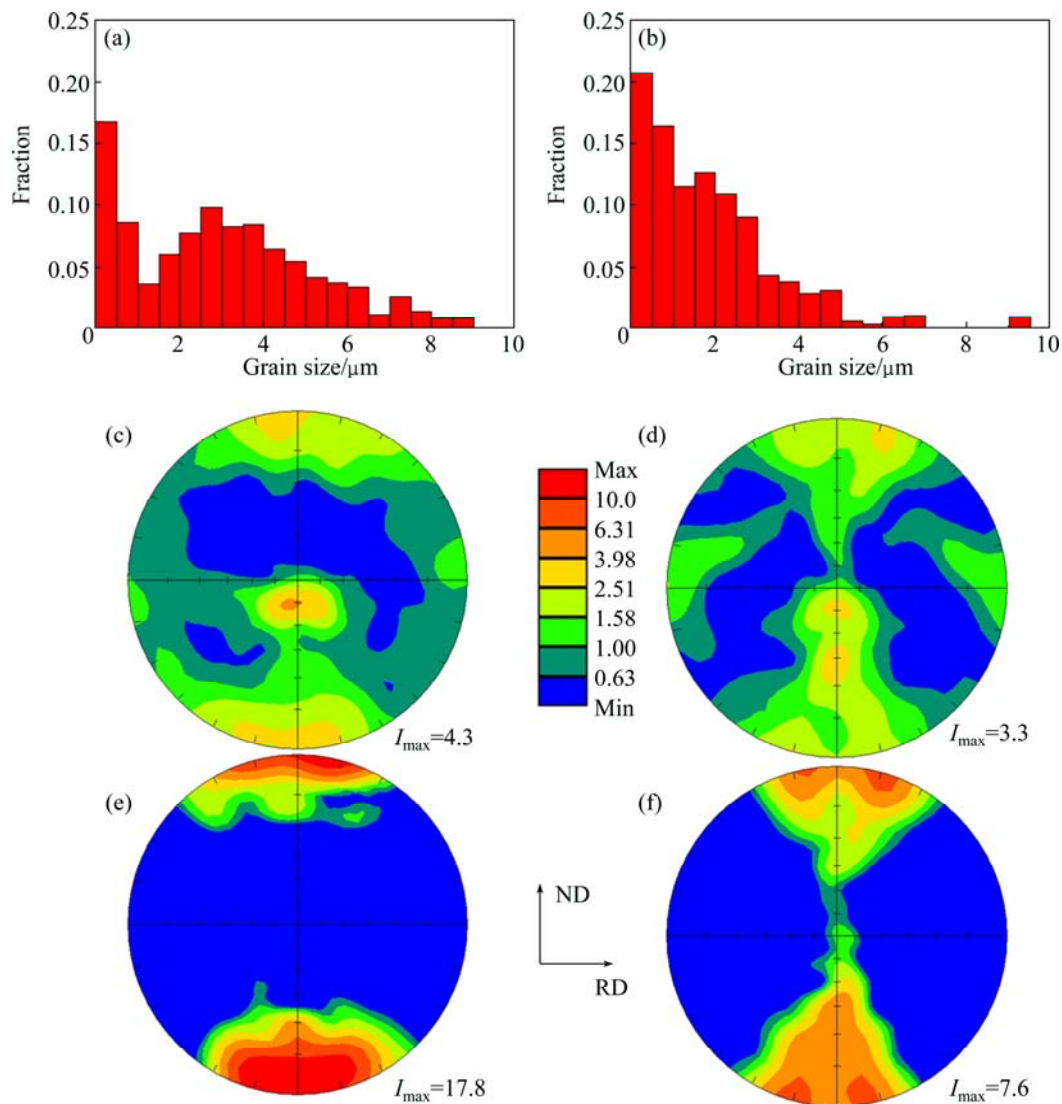


Fig. 7 Effects of PSN and Ca addition on texture alteration in AM60-0.8 (a, c, e) and ZX200 (b, d, f) sheets: (a, b) Grain size distribution; (c, d) (0002) pole figures for grains less than 1 μm ; (e, f) (0002) pole figure for grains greater than 1 μm

oriented nuclei in Mg alloys [17] and Al alloys [21]. However, Fig. 7(c) shows that the fine recrystallized grains have particular preferred orientations but not random orientations, although some of them formed by PSN. It is noted that, the previously reported texture analysis associated with PSN was usually produced in the materials after extrusion and/or the subsequent annealing. In our case, however, the multi-pass hot rolling was adopted. The subsequent rolling process after the formation of recrystallized grains would also make these grains rotate again and then alter their original random orientations. But interestingly, these fine grains also do not obtain a strong basal texture similar to the large grains (Fig. 7(e)), but rather a texture feature with *c*-axis parallel to TD, ND and RD (Fig. 7(c)). One of the possible reasons is that these fine grains are too small to be favorable for the activity of twinning [22] in which, in particular, tensile twinning may promote a rapid

reorientation of grains and have a considerable contribution to the formation of basal texture [9,23]. Another reason is that those fine particles would suppress the rotation of those recrystallized grains and thus, have a potential influence on the formation of preferably oriented grains. Additionally, the matrix orientation and strain distribution in the deformation zone around particles would also have a non-negligible effect on the orientations of recrystallized grains [24,25].

As compared with Y or RE elements, Ca additions are quite cheap, and also they can significantly improve the creep and oxidation resistances [26,27]. Therefore, it is interest to investigate the potential promotion of Ca additions in Mg alloys to the texture alteration and sheet formability. It is noted that, the possible texture-altering mechanisms may be different for Ca- and RE-containing alloys. For example, only few particles precipitated in RE-containing alloys [9] but extensive particles in

ZXM200 alloy (Fig. 5(b)). In this regard, more detailed investigations should be conducted in the future work.

As discussed above, due to the effect of fine recrystallized grains and/or Ca addition, both the as-rolled AM60-0.8 and ZXM200 sheets show different crystallographic textures from that observed in AM60-2. However, AM60-0.8 sheet exhibits a similar mechanical anisotropy to AM60-2, while ZXM200 exhibits different anisotropic characteristics from AM60-2. As seen from Figs. 7(c) and (e), this texture alteration in AM60-0.8 is totally attributed to those fine recrystallized grains; while in addition to the effect of these fine grains, Ca addition also has a significant contribution to the texture alteration in ZXM200. Thus, it seems that Ca addition is responsible for the change of mechanical anisotropy. It is noted that, Ca addition mainly alters the texture features of large grains. The texture alteration of these large grains makes some grains have a better aligned orientation for the formation of twinning as the specimen is tested at a given tensile direction, while twins cannot form in these grains at all during another direction tensile test due to the strong sensitivity of twinning on the applied loading [28]. This leads to different yield strength and elongation when the tension is tested at different loading directions, i.e. the mechanical anisotropy. However, due to their smaller size, the fine recrystallized grains are not favorable for the formation of twinning even though they have a better aligned orientation. Therefore, the texture alteration resulted from fine recrystallized grains has less effect on the change of mechanical anisotropy.

4 Conclusions

1) The addition of Ca to magnesium alloy followed by a multi-pass hot rolling produces some particles that are Mg–Ca binary phase or Mg–Zn–Ca ternary phase. Some finer recrystallized grains exist in the rolled Mg–Zn–Ca sheet, but not all of them are formed through PSN.

2) In rolled Mg–Zn–Ca sheets, the fine recrystallized grains usually exhibit three preferred orientations with *c*-axis parallel to TD, ND and RD, which may help the texture alteration in rolled Mg sheets, but have a slight effect on the mechanical anisotropy.

3) The solid solution of Ca into Mg matrix may promote the formation of texture component with *c*-axis rotated away from ND towards TD and then weaken the overall texture intensity, which has a similar influence on the texture alteration to RE-containing Mg alloys. That is, the addition of Ca to magnesium alloys has the potential to substitute for RE elements in weakening the strong texture of Mg sheets.

Acknowledgements

The authors are grateful for helpful discussion with Dr Tomoyuki HOMMA, NUT, Japan. Valuable comments from the reviewer are also gratefully acknowledged.

References

- [1] HUANG X S, SUZUKI K, SAITO N. Enhancement of stretch formability of Mg–3Al–1Zn alloy sheet using hot rolling at high temperatures up to 823 K and subsequent warm rolling [J]. *Scripta Mater*, 2009, 61: 445–448.
- [2] HUANG X S, SUZUKI K, WATAZU A, SHIGEMATSU I, SAITO N. Mechanical properties of Mg–Al–Zn alloy with a tilted basal texture obtained by differential speed rolling [J]. *Mater Sci Eng A*, 2008, 488: 214–220.
- [3] CHINO Y, SASSA K, KAMIYA A, MABUCHI M. Stretch formability at elevated temperature of a cross-rolled AZ31 Mg alloy sheet with different rolling routes [J]. *Mater Sci Eng A*, 2008, 473: 195–200.
- [4] CHINO Y, SASSA K, KAMIYA A, MABUCHI M. Enhanced formability at elevated temperature of a cross-rolled magnesium alloy sheet [J]. *Mater Sci Eng A*, 2006, 441: 349–356.
- [5] LASER T, HARTIG C H, NÜRNBERG M R, LETZIG D, BORMANN R. The influence of calcium and cerium mischmetal on the microstructural evolution of Mg–3Al–1Zn during extrusion and resulting mechanical properties [J]. *Acta Mater*, 2008, 56: 2791–2798.
- [6] KIM W J, LEE J B, KIM W Y, JEONG H T, JEONG H G. Microstructure and mechanical properties of Mg–Al–Zn alloy sheets severely deformed by asymmetrical rolling [J]. *Scripta Mater*, 2007, 56: 309–312.
- [7] BALL E A, PRANGNELL P B. Tensile-compressive yield asymmetries in high strength wrought magnesium alloys [J]. *Scripta Metall Mater*, 1994, 31: 111–116.
- [8] AGNEW S R, SENN J W, HORTON J A. Mg sheet metal forming: Lessons learned from deep drawing Li and Y solid-solution alloys [J]. *JOM*, 2006, 58: 62–69.
- [9] BOHLEN J, NÜRNBERG M R, SENN J, LETZIG D, AGNEW S R. The texture and anisotropy of magnesium-zinc-rare earth alloy sheets [J]. *Acta Mater*, 2007, 55: 2101–2112.
- [10] STANFORD N, BARNETT M. Effect of composition on the texture and deformation behaviour of wrought Mg alloys [J]. *Scripta Mater*, 2008, 58: 179–182.
- [11] PÉREZ-PRADO M T, DEL VALLE J A, CONTRERAS J M, RUANO O A. Microstructural evolution during large strain hot rolling of an AM60 Mg alloy [J]. *Scripta Mater*, 2004, 50: 661–665.
- [12] STYCZYNSKI A, HARTIG C H, BOHLEN J, LETZIG D. Cold rolling textures in AZ31 wrought magnesium alloy [J]. *Scripta Mater*, 2004, 50: 943–947.
- [13] NAN X L, WANG H Y, ZHANG L, LI J B, JIANG Q C. Calculation of Schmid factors in magnesium: Analysis of deformation behaviors [J]. *Scripta Mater*, 2012, 67: 443–446.
- [14] JARDIM P M, SOLÓRZANO G, VANDER SANDE J B. Second phase formation in melt-spun Mg–Ca–Zn alloys [J]. *Mater Sci Eng A*, 2004, 381: 196–205.
- [15] BETTLES C J, GIBSON M A, VENKATESAN K. Enhanced age-hardening behaviour in Mg–4wt.%Zn micro-alloyed with Ca [J]. *Scripta Mater*, 2004, 51: 193–197.
- [16] OH-ISHI K, WATANABE R, MENDIS C L, HONO K. Age-hardening response of Mg–0.3 at.%Ca alloys with different Zn contents [J]. *Mater Sci Eng A*, 2009, 526: 177–184.
- [17] ROBSON J D, HENRY D T, DAVIS B. Particle effects on

- recrystallization in magnesium–manganese alloys: Particle-stimulated nucleation [J]. *Acta Mater*, 2009, 57: 2739–2747.
- [18] PARK S H, YU H, BAE J H, YIM C D, YOU B S. Microstructural evolution of indirect-extruded ZK60 alloy by adding Ce [J]. *J Alloy Compd*, 2012, 545: 139–143.
- [19] KYEONG J S, KIM J K, LEE M J, PARK Y B, KIM W T, KIM D H. Texture modification by addition of Ca in Mg–Zn–Y alloy [J]. *Mater Trans*, 2012, 53: 991–994.
- [20] STANFORD N. The effect of calcium on the texture, microstructure and mechanical properties of extruded Mg–Mn–Ca alloys [J]. *Mater Sci Eng A*, 2010, 528: 314–322.
- [21] HUMPHREYS F J. The nucleation of recrystallization at second phase particles in deformed aluminum [J]. *Acta Metall Mater*, 1977, 25: 1323–1344.
- [22] WANG J T, YIN D L, LIU J Q, TAO J, SU Y L, ZHAO X. Effect of grain size on mechanical property of Mg–3Al–1Zn alloy [J]. *Scripta Mater*, 2008, 59: 63–66.
- [23] BROWN D W, AGNEW S R, BOURKE M A M, HOLDEN T M, VOGEL S C, TOMÉ C N. Internal strain and texture evolution during deformation twinning in magnesium [J]. *Mater Sci Eng A*, 2005, 399: 1–12.
- [24] ENGLER O, KONG X W, LÜCKE K. Recrystallisation textures of particle-containing Al–Cu and Al–Mn single crystals [J]. *Acta Mater*, 2001, 49: 1701–1715.
- [25] SCHÄFER C, SONG J, GOTTSTEIN G. Modeling of texture evolution in the deformation zone of second-phase particles [J]. *Acta Mater*, 2009, 57: 1026–1034.
- [26] ZHU S M, MORDIKE B L, NIE J F. Creep properties of a Mg–Al–Ca alloy produced by different casting technologies [J]. *Mater Sci Eng A*, 2008, 483–484: 583–586.
- [27] NINOMIYA R, OJIRO T, KUBOTA K. Improved heat resistance of Mg–Al alloys by the Ca addition [J]. *Acta Metall Mater*, 1995, 43: 669–674.
- [28] BARNETT M R. Twinning and the ductility of magnesium alloys. Part I: “Tension” twins [J]. *Mater Sci Eng A*, 2007, 464: 1–7.

Ca 添加对镁合金板材组织和织构的影响

丁汉林¹, 张鹏², 程广萍¹, Shigeharu KAMADO³

1. 安徽工业大学 材料科学与工程学院, 马鞍山 243002;

2. 上海交通大学 轻合金精密成型国家工程研究中心, 上海 200030;

3. Department of Mechanical Engineering, Nagaoka University of Technology, Niigata 940-2188, Japan

摘要: 采用多道次轧制方法制备 AM60 (Mg–6.0Al–0.3Mn, 质量分数%)和 ZXM200 (Mg–1.6Zn–0.5Ca–0.2Mn) 镁合金板材, 并研究镁合金板材的力学性能和织构特征。研究表明, 在添加 Ca 的镁合金轧板中, 细小的再结晶晶粒表现出特定的取向特征, 从而改变了轧板的整体织构特征; 固溶至镁基体中的 Ca 元素促使晶粒 *c* 轴由板坯法线方向向板宽方向偏转, 亦可明显弱化板材织构。这导致了含 Ca 的镁合金板材表现出与稀土镁合金类似的织构特征。

关键词: 镁板; 热轧; 动态再结晶; Ca 添加; 织构弱化

(Edited by Xiang-qun LI)